AD

TECHNICAL REPORT ARCCB-TR-99004

LASER-ULTRASONIC CHARACTERIZATION OF ELECTRODEPOSITED CHROMIUM COATINGS

BRYON KNIGHT
JEFFREY BRAUNSTEIN
JOSEPH F. COX
JULIUS FRANKEL

MARCH 1999

US ARMY ARMAMENT RESEARCH, DEVELOPMENT AND ENGINEERING CENTER
CLOSE COMBAT ARMAMENTS CENTER
BENÉT LABORATORIES
WATERVLIET, N.Y. 12189-4050

APPROVED FOR PUBLIC RELEASE; DISTRIBUTION UNLIMITED

19990422 009

DISCLAIMER

The findings in this report are not to be construed as an official Department of the Army position unless so designated by other authorized documents.

The use of trade name(s) and/or manufacturer(s) does not constitute an official endorsement or approval.

DESTRUCTION NOTICE

For classified documents, follow the procedures in DoD 5200.22-M, Industrial Security Manual, Section II-19, or DoD 5200.1-R, Information Security Program Regulation, Chapter IX.

For unclassified, limited documents, destroy by any method that will prevent disclosure of contents or reconstruction of the document.

For unclassified, unlimited documents, destroy when the report is no longer needed. Do not return it to the originator.

REPORT DOCUMENTATION PAGE

Public reporting burden for this collection of information is estimated to average 1 hour per response, including the time for reviewing instructions, searching existing data sources, gathering and maintaining the data needed, and completing and reviewing the collection of information. Send comments regarding this burden estimate or any other aspect of this collection of information, including suggestions for reducing this burden, to Washington Headquarters Services, Directorate for Information Operations and Reports, 1215 Jefferson Davis Highway, Suite 1204, Arlington, VA 22202-4302, and to the Office of Management and Budget, Paperwork Reduction Project (0704-0188), Washington, DC 20503.

1. AGENCY USE ONLY (Leave blank)	2. REPORT DATE March 1999	3. REPORT TYPE AND DATES COVERED Final

4. TITLE AND SUBTITLE

LASER-ULTRASONIC CHARACTERIZATION OF ELECTRODEPOSITED CHROMIUM COATINGS

5. FUNDING NUMBERS

AMCMS No. 6111.01.91A1.1

6. AUTHOR(S)

Bryon Knight, Jeffrey Braunstein, Joseph F. Cox, and Julius Frankel

7. PERFORMING ORGANIZATION NAME(S) AND ADDRESS(ES)

U.S. Army ARDEC
Benet Laboratories, AMSTA-AR-CCB-O
Watervliet, NY 12189-4050

8. PERFORMING ORGANIZATION REPORT NUMBER

ARCCB-TR-99004

9. SPONSORING / MONITORING AGENCY NAME(S) AND ADDRESS(ES)

U.S. Army ARDEC
Close Combat Armaments Center
Picatinny Arsenal, NJ 07806-5000

10. SPONSORING / MONITORING AGENCY REPORT NUMBER

11. SUPPLEMENTARY NOTES

Presented at the 23rd Conference on Quantitative Non-Destructive Evaluation, Snowbird, UT, 23 July 1998.
Published in proceedings of the conference.

12a. DISTRIBUTION / AVAILABILITY STATEMENT

Approved for public release; distribution unlimited.

12b. DISTRIBUTION CODE

13. ABSTRACT (Maximum 200 words)

Chromium coatings were electrodeposited onto steel substrates, under controlled conditions. A pulsed laser generated ultrasonic waves in the specimen, and a Michelson interferometer detected the ultrasonic waves at the surface. Signal processing techniques were used to obtain the surface wave velocities, and the various modes are discussed. Conventional piezoelectric techniques were also used for generation and detection of bulk wave velocities to correlate with the surface wave results. A difference technique was used to obtain the bulk measurements: time transit and thickness were measured before and after chromium plating and the velocities evaluated from the respective differences of the data thus obtained.

14. SUBJECT TERMS

Ultrasonics, Laser-Ultrasonics, Elastic Properties, Coatings

15. NUMBER OF PAGES

12

16. PRICE CODE

17. SECURITY CLASSIFICATION OF REPORT	18. SECURITY CLASSIFICATION OF THIS PAGE	19. SECURITY CLASSIFICATION OF ABSTRACT	20. LIMITATION OF ABSTRACT
UNCLASSIFIED	UNCLASSIFIED	UNCLASSIFIED	UL

NSN 7540-01-280-5500

TABLE OF CONTENTS

TABLES

LIST OF ILLUSTRATIONS

ACKNOWLEDGEMENTS

INTRODUCTION

Metal coatings are of interest in applications where erosion, corrosion, or mechanical degradation results from chemical, temperature, and mechanical insults to the surface. The evaluation of a coating nondestructively responds to the need to estimate its effectiveness prior to actual use, without damaging it. An area of interest is the coatings' elastic properties. These properties were determined here by measuring bulk and Rayleigh ultrasonic velocities. The material bulk velocities were found by measuring the thickness and shear and longitudinal ultrasonic time-of-flight of the substrate, with and without the electroplated chromium coating. Elastic properties of the material were calculated from the bulk velocities measured, assuming little or no dispersion within the material. The Rayleigh—surface wave—velocity was measured using a pulsed laser for ultrasonic wave generation in conjunction with a Michelson interferometer for signal detection. Wavelet analysis was used as a signal-processing technique to determine the dispersion curves for the laser-generated surface acoustic waves. The specimens were produced by electrodepositing chromium of various thicknesses on 2 in. x 1 in. x 0.5 in. steel coupons using controlled plating parameters.

THEORY

An elastic disturbance, ξ_x, traveling through an isotropic material along the x-axis can be described by the wave equation

$$\frac{\partial^2 \xi_x}{\partial t^2} = V^2 \frac{\partial^2 \xi_x}{\partial x^2} \tag{1}$$

where V is the sound velocity. The wave equations for longitudinal and shear waves are functions of three material properties: Young's modulus, E, Poisson's ratio, v, and the material density, ρ. The longitudinal wave equation is

$$\frac{\partial^2 \xi_x}{\partial t^2} = \left(\frac{E(1-v)}{\rho(1+v)(1-2v)} \right) \frac{\partial^2 \xi_x}{\partial x^2} \tag{2}$$

and therefore, the longitudinal velocity, V_l, is

$$V_l = \sqrt{\frac{E(1-v)}{\rho(1+v)(1-2v)}} \tag{3}$$

The shear wave equation is

$$\frac{\partial^2 \xi_x}{\partial t^2} = \left(\frac{E}{2\rho(1+v)} \right) \frac{\partial^2 \xi_x}{\partial y^2} \tag{4}$$

and the shear velocity, V_t, is shown as

1

$$V_t = \sqrt{\frac{E}{2\rho(1+\nu)}} \qquad (5)$$

A Rayleigh wave is a surface wave that contains components of both shear and longitudinal waves and its velocity, V_R, is

$$V_R = V_t\left(\frac{0.87+1.13\nu}{1+\nu}\right) \qquad (6)$$

Young's modulus is calculated from the bulk shear and longitudinal velocities (assuming negligible dispersion), and the density

$$E = \rho V_t^2\left(\frac{3V_l^2 - 4V_t^2}{V_l^2 - V_t^2}\right) \qquad (7)$$

and Poisson's ratio

$$\nu = \frac{V_l^2 - 2V_t^2}{2(V_l^2 - V_t^2)} \qquad (8)$$

are dependent on the longitudinal and shear velocities alone.

EXPERIMENT

Specimen Preparation

Chromium coatings were electrodeposited on ASTM A723 steel coupons from aqueous solutions containing 250 g/l CrO_3 and 2.5 g/l H_2SO_4. Deposition was at a rate of 0.02 mm/hr with the bath temperature and the current density maintained at constant values. The steel substrates were first mechanically cleaned, then electrocleaned in strong caustic solution, and finally rinsed in demineralized water immediately prior to insertion in the plating bath.

Surface Wave Measurements

Ultrasonic surface waves are generated in the thermoelastic regime by pulses of an Nd:YAG laser (70 mj, 8 nsec pulse width) impinging normally and in a 1-in. diameter circle on the surface (see Figure 1). The width of the laser beam at the specimen is 0.005 to 0.01 in. Note that surface waves with frequencies into the 30 MHz range are generated. The Rayleigh waves effectively die out within one wavelength of the surface, so that frequencies larger than V_R/x, where x is the thickness of the coating, can be used to characterize the coating and frequencies lower than V_R/x, the substrate. The thinner the coating the higher the frequencies needed to propagate surface waves within the coating. Further, since the chromium velocities are slightly higher than those for steel, the arrival of the higher frequency signal (coating) precedes that of the lower frequency one (substrate).

Beam shape at various stages

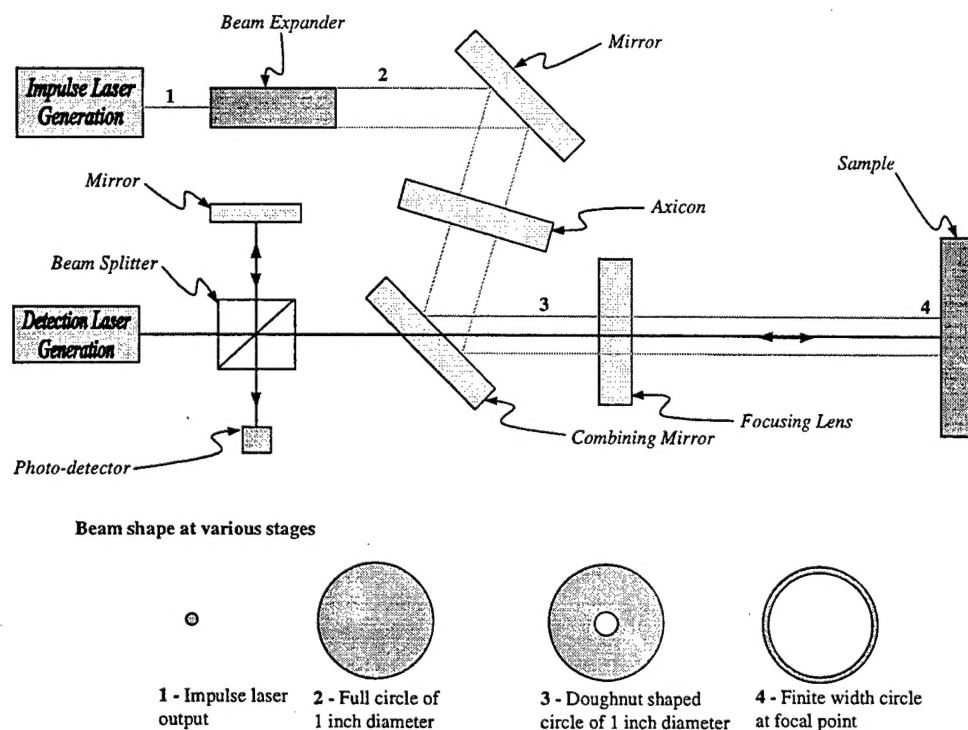| 1 - Impulse laser output | 2 - Full circle of 1 inch diameter | 3 - Doughnut shaped circle of 1 inch diameter | 4 - Finite width circle at focal point |

Figure 1. Laser system, including Michelson interferometer and laser generation.

A Michelson optical interferometer (ref 1) measures the instantaneous displacement of a surface based upon interference between the superposition of two or more monochromatic beams of light. It uses two beams: a signal leg (moving) and a reference leg (static), and measures the phase between the two beams. The reference leg is a beam that travels to a fixed mirror and back, and the signal leg is a beam that reflects off the surface of the sample, as seen in Figure 1. A 10 mW HeNe CW laser of 632.8 nm provides the light source; this source is divided into the reference and signal legs by a beam splitter. The beam splitter also recombines the two beams, which then impinge on a photodetector. The resultant beam intensity detected at the photodetector depends on the phase difference between the reference and signal beams. If the difference in phase is less than one-half of a wavelength, constructive interference occurs and the intensity is increased. Destructive interference occurs when there is a difference of more than one-half of a wavelength between the beams, therefore the intensity is decreased. The displacement at the surface is then correlated to the difference in phase between the two beams.

In our study, waveforms were accumulated with a Sonix STR 81G 8-bit digitizing card installed in a PC and controlled with a LabVIEW program. The LabVIEW program was used to obtain and save the ultrasonic data. The data contained 8192 points and was digitized at 1 GHz (real-time sampling). Each waveform was made up of the average of 200 individual waveforms. A phase compensating routine was used, as the Michelson interferometer was not phase stabilized.

Application of Wavelets to Obtain Dispersion Curves

Wavelet analysis (refs 2-4) was applied to the Rayleigh wave signals, to determine the frequency-velocity (dispersion) relationship. The frequency and velocity relationships were extracted from the contour map resulting from the wavelet transformation. The frequency was determined from the frequency transform of the mother wavelet and subsequently adapted for the scales associated with the daughter wavelets. A wavelet transform was applied to the signal in the frequency domain. The test wavelet consisted of a Gaussian function, equivalent to a Morlet wavelet, located about a center frequency.

Initially, the Fourier transform was applied to the laser-generated data in order to carry out the computation in the frequency domain. Then the inverse Fourier transform of the product of the wavelet and the laser data was generated. Explicit control of the wavelet bandwidth was necessary to improve the quality of the wavelet transform. The latter is very dependent on the wavelet bandwidth. Applying the method to a test case with a Gaussian modulated linear chirp showed that when the bandwidth was too large, the high frequency components of the wavelet transform were very inaccurate. An additional difficulty was observed with the laser data, since the frequencies present were very small relative to the sampling rate, bandwidths that were too small introduced substantial numerical noise into the transform.

Determining the velocity introduced the greatest uncertainty. The association between frequency and velocity is dependent on the relationship between scale and time in the wavelet decomposition. Having determined the frequency associated with scale and determined the velocity from the radius of the circle and the time of arrival, it was necessary to determine the point that had the highest correlation to determine the dispersion curve. For a given scale, the time of arrival was determined by taking the centroid of the 10 points with the largest wavelet coefficients. Other methods were considered, such as using the point with the maximum wavelet coefficient, or using the mean time of the 10 points. The single point method was not used due to the noise that was observed at high frequencies. The data quality would diminish and an averaging scheme would be necessary to determine the time of arrival. The centroid method was chosen over the mean time because it allowed weighing the data to best determine the time of arrival. The dispersion curves can be seen in Figure 2.
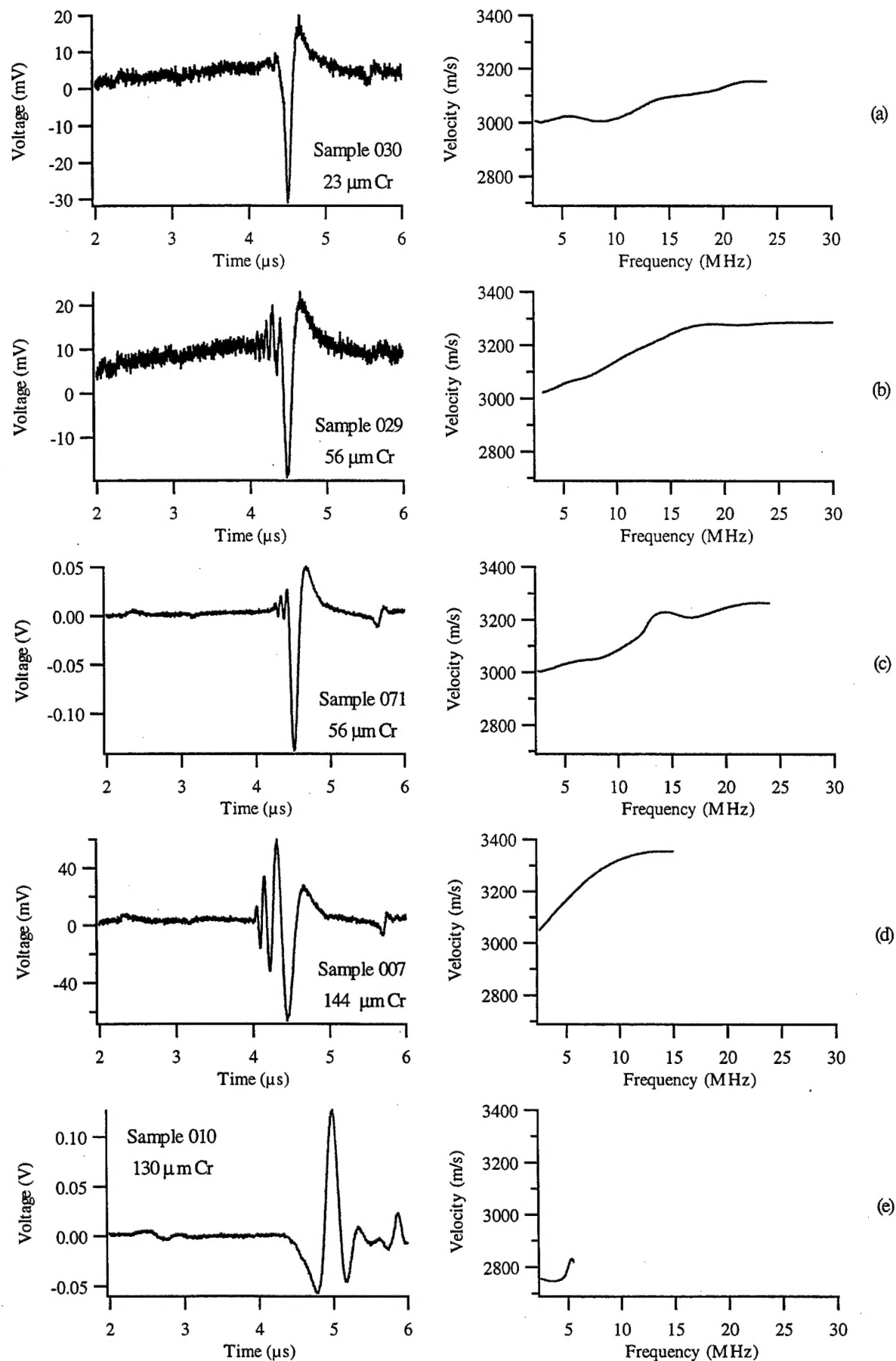
Figure 2. Waveforms from laser-generated surface waves (left)
and their corresponding dispersion curves (right).

Bulk Wave Measurements

Bulk velocities for shear and longitudinal modes for the coating are obtained by a difference technique. Figure 3 shows the system setup. The thickness and ultrasonic pulse transit time are measured for the chromium coated steel specimen. The coating is then removed and the measurements are repeated. Longitudinal and shear transducers of 5 and/or 10 MHz of 0.25 inch in diameter are used for the time-of-flight measurements. To avoid near field effects of the transducers, a buffer is used in the ultrasonic measurements. The thickness is measured with a micrometer to within 3×10^{-5} inches and the time-of-flight to ± 1.5 nsec. The bulk velocities in the chromium coating, $V_{chromium}$, are calculated as

$$V_{chromium} = \frac{2(x_{total} - x_{steel})}{\Delta t_{total} - \Delta t_{steel}} \tag{9}$$

where x_{total} and Δt_{total} are the thickness and ultrasonic travel time, respectively, for the chromium coated sample, and x_{steel} and Δt_{steel} are the thickness and ultrasonic travel time, respectively, for the specimen after the coating has been removed.
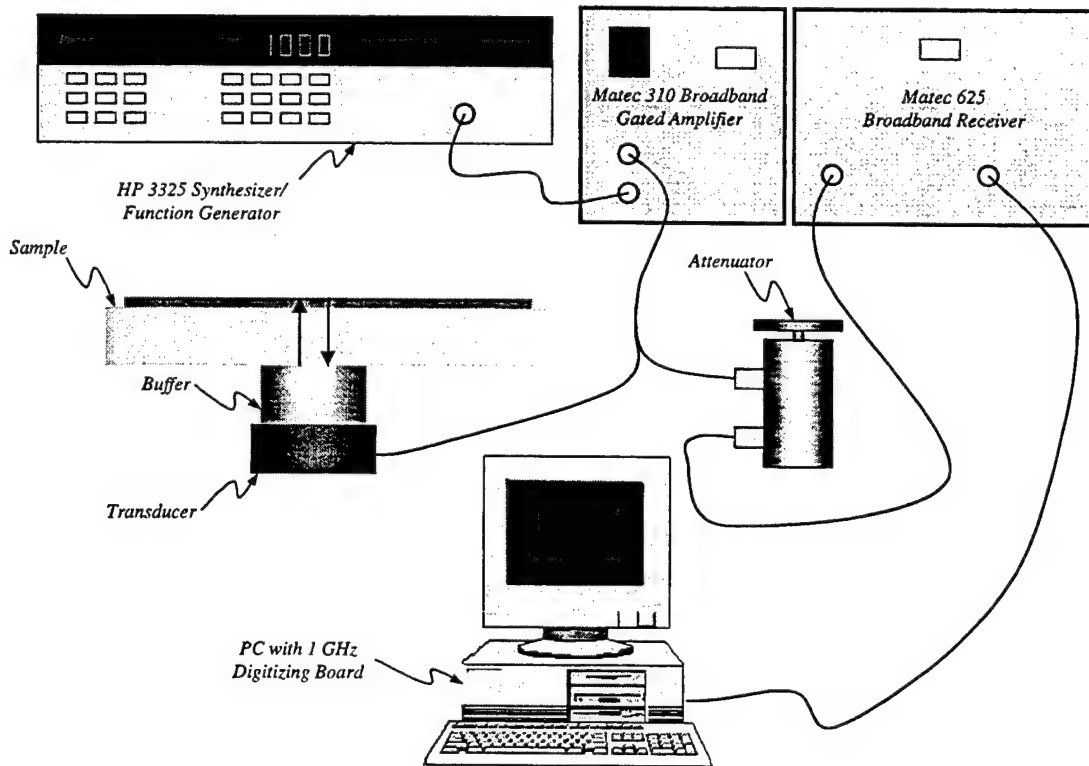

Figure 3. System for bulk ultrasonic velocity measurements.

As above, waveforms were accumulated with a Sonix STR 81G 8-bit digitizing card installed in a PC and controlled with a LabVIEW program. The LabVIEW program was used to obtain and process the time-of-flight data. The digitizer was set to a sampling rate of 1 GHz (real time), each waveform contained 8192 samples, and a measurement included the average of 256 individual waveforms. Ten measurements were averaged (a total of 2560 waveforms) for each set of specimen conditions. Cross correlation and peak detection virtual instruments (VIs) incorporated in the LabVIEW program were used to obtain times-of-flight from the waveforms, using the first and second back-surface echoes.

DISCUSSION AND RESULTS

Rayleigh wave velocity measurements were made on five chromium plated specimens. The chromium coatings were 144, 130, 56, 56, and 23 microns thick. The waveforms from the interferometer surface displacement measurements and the resulting dispersion curves for each sample are shown in Figure 2. Rayleigh wave velocities were also calculated from the bulk wave velocity measurements made on two samples: 144 μm chromium (sample 007) and 130 μm chromium (sample 010). For coatings thicker than about 125 μm, the difference technique used to obtain longitudinal and shear wave velocities resulted in an error (standard deviation) of less than ±4 percent. The measurement error increased rapidly as the coating thickness decreased.

The results of bulk longitudinal and shear velocity measurements made on samples 007 and 010 are shown in Table 1. The measured values of coating thickness and calculated values of Poisson's ratio, Rayleigh velocity, and Young's modulus are also included. The literature values in Table 1 are compiled as a result of the Hashin and Shtrikman method (ref 5) for bulk chromium.

Table 1. Chromium Coating Properties for Samples 007 and 010

	Sample 007	Sample 010	Literature Values (ref 5)
Thickness (μm)	144	130	--
Longitudinal Velocity (m/s)	6040	6419	6622
Shear Velocity (m/s)	3404	2983	4002
Rayleigh Velocity (calculated) (m/s)	3148	2801	3664
Rayleigh Velocity (measured) (m/s)	3360	Not present	3664
Poisson's Ratio	0.267	0.360	0.212
Young's Modulus (Gpa)	211	175	276

The Rayleigh wave characteristics of coatings depend on the coating thickness. The frequency of the Rayleigh wave in the chromium coating increases with decreasing coating thickness, and its characteristic signal arrives earlier than that for steel. Dispersion curves for the Rayleigh velocities were obtained through wavelet analysis of the laser ultrasonic waveforms. For sample 030 we would expect the chromium Rayleigh velocity to appear around 140 MHz, for the other coating thicknesses, around 60 and 22 MHz, respectively. The dispersion curve showed gently rising values, which had not reached the coating thickness; hence, for the in-between frequencies, the observed velocities showed the effect of both coating and substrate in proportion to the ratio of coating thickness to wavelength. The two 56 μm coatings revealed similar features and also gently rising slopes. The steepest slope was found for 007 with the 144 μm coating thickness. Specimens 007 and 010 showed a substantial difference even though they were plated under identical parameters, to almost identical thickness. The first clue was the Rayleigh signal itself, which showed no chromium arrival for sample 010. The dispersion curve showed no higher frequencies, and the velocity at lower frequency (which should be the steel value) did not resemble the value found for steel in the other specimens. The frequency range established for the dispersion curves for all the samples was dictated by the signal-to-noise ratio at the higher frequencies. The micrographs of these last two specimens, presented in Figure 4, do indeed show that sample 010 had a crack at the chromium-steel interface. The results of our bulk wave measurements also revealed a substantial difference between the two specimens. The most glaring difference between the two was the Poisson's ratio, which differed by about 40 percent.
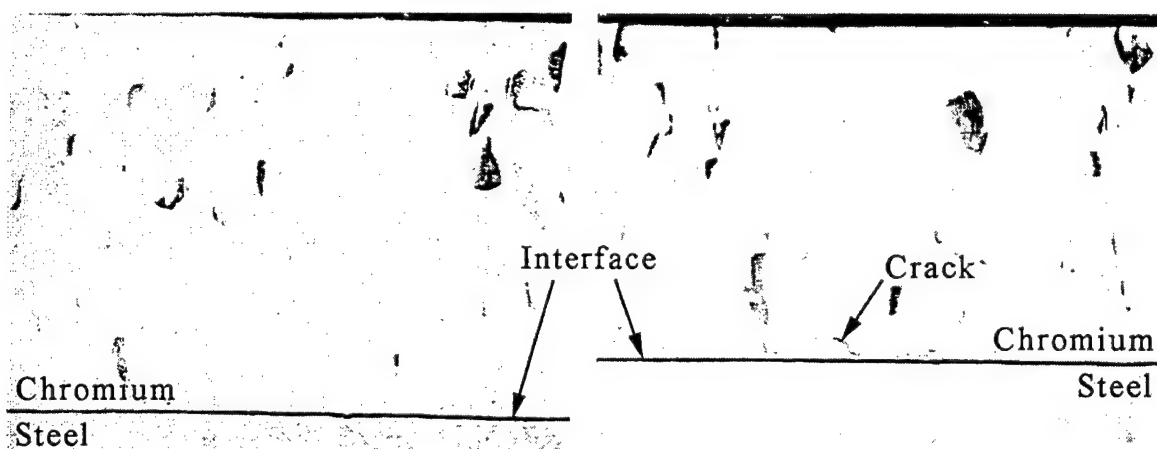

Figure 4. Micrographs of chromium coatings for
sample 010 (right) at 500x and sample 007 (left) at 500x.

CONCLUSIONS

The Rayleigh wave characteristics of chromium electrodeposited onto steel coupons depend on the thickness and on the elastic properties and quality of the electrodeposit. Dispersion curves and Rayleigh velocities can be obtained through wavelet analysis of the laser ultrasonic waveforms. We found a substantial variation in the properties of two chromium coatings of similar thickness prepared under carefully controlled and apparently identical plating conditions, as seen in Table 1, and these differed from bulk values for pure chromium found in the literature.

REFERENCES

1. "LaserWave" communications provided by Textron Systems Division, 201 Lowell Street, Wilmington, MA 01887-2941.

2. Abbate, A., Frankel, J., and Das, P., "Wavelet Transfrom Signal Processing for Dispersion Analysis of Ultrasonic Signals," *1995 IEEE Ultrasonic Symposium Proceedings*, pp. 751-755.

3. Abbate, A., Koay, J., Frankel, J., Schroeder, S.C., and Das, P., "Application of Wavelet Transform Signal Processing to Ultrasound," *1994 IEEE Ultrasonic Symposium Proceedings*, pp. 1147-1152.

4. Abbate, A., Frankel, J., and Das, P., "Wavelet Transform Signal Processing Applied to Ultrasonics,", *Review of Progress in QNDE*, Vol. 15, (D.O. Thompson and D.E. Chimenti, Eds.), Plenum, NY, 1996, pp. 741-748.

5. Simmons, G., and Wang, H., *Single Crystal Elastic Constants and Calculated Aggregate Properties: A Handbook*, The M.I.T. Press, Cambridge, 1971.

TECHNICAL REPORT INTERNAL DISTRIBUTION LIST

	NO. OF COPIES
CHIEF, DEVELOPMENT ENGINEERING DIVISION	
ATTN: AMSTA-AR-CCB-DA	1
-DB	1
-DC	1
-DD	1
-DE	1
CHIEF, ENGINEERING DIVISION	
ATTN: AMSTA-AR-CCB-E	1
-EA	1
-EB	1
-EC	1
CHIEF, TECHNOLOGY DIVISION	
ATTN: AMSTA-AR-CCB-T	2
-TA	1
-TB	1
-TC	1
TECHNICAL LIBRARY	
ATTN: AMSTA-AR-CCB-O	5
TECHNICAL PUBLICATIONS & EDITING SECTION	
ATTN: AMSTA-AR-CCB-O	3
OPERATIONS DIRECTORATE	
ATTN: SIOWV-ODP-P	1
DIRECTOR, PROCUREMENT & CONTRACTING DIRECTORATE	
ATTN: SIOWV-PP	1
DIRECTOR, PRODUCT ASSURANCE & TEST DIRECTORATE	
ATTN: SIOWV-QA	1

NOTE: PLEASE NOTIFY DIRECTOR, BENÉT LABORATORIES, ATTN: AMSTA-AR-CCB-O OF ADDRESS CHANGES.

TECHNICAL REPORT EXTERNAL DISTRIBUTION LIST

	NO. OF COPIES		NO. OF COPIES
DEFENSE TECHNICAL INFO CENTER ATTN: DTIC-OCA (ACQUISITIONS) 8725 JOHN J. KINGMAN ROAD STE 0944 FT. BELVOIR, VA 22060-6218	2	COMMANDER ROCK ISLAND ARSENAL ATTN: SIORI-SEM-L ROCK ISLAND, IL 61299-5001	1
COMMANDER U.S. ARMY ARDEC ATTN: AMSTA-AR-WEE, BLDG. 3022 AMSTA-AR-AET-O, BLDG. 183 AMSTA-AR-FSA, BLDG. 61 AMSTA-AR-FSX AMSTA-AR-FSA-M, BLDG. 61 SO AMSTA-AR-WEL-TL, BLDG. 59 PICATINNY ARSENAL, NJ 07806-5000	1 1 1 1 1 2	COMMANDER U.S. ARMY TANK-AUTMV R&D COMMAND ATTN: AMSTA-DDL (TECH LIBRARY) WARREN, MI 48397-5000	1
DIRECTOR U.S. ARMY RESEARCH LABORATORY ATTN: AMSRL-DD-T, BLDG. 305 ABERDEEN PROVING GROUND, MD 21005-5066	1	COMMANDER U.S. MILITARY ACADEMY ATTN: DEPT OF CIVIL & MECH ENGR WEST POINT, NY 10966-1792	1
DIRECTOR U.S. ARMY RESEARCH LABORATORY ATTN: AMSRL-WM-MB (DR. B. BURNS) ABERDEEN PROVING GROUND, MD 21005-5066	1	U.S. ARMY AVIATION AND MISSILE COM REDSTONE SCIENTIFIC INFO CENTER ATTN: AMSAM-RD-OB-R (DOCUMENTS) REDSTONE ARSENAL, AL 35898-5000	2
COMMANDER U.S. ARMY RESEARCH OFFICE ATTN: TECHNICAL LIBRARIAN P.O. BOX 12211 4300 S. MIAMI BOULEVARD RESEARCH TRIANGLE PARK, NC 27709-2211	1	COMMANDER U.S. ARMY FOREIGN SCI & TECH CENTER ATTN: DRXST-SD 220 7TH STREET, N.E. CHARLOTTESVILLE, VA 22901	1

NOTE: PLEASE NOTIFY COMMANDER, ARMAMENT RESEARCH, DEVELOPMENT, AND ENGINEERING CENTER, BENÉT LABORATORIES, CCAC, U.S. ARMY TANK-AUTOMOTIVE AND ARMAMENTS COMMAND, AMSTA-AR-CCB-O, WATERVLIET, NY 12189-4050 OF ADDRESS CHANGES.